JASS Journal of Astronomy and Space Sciences

Do Solar Cycles Share Spectral Properties with Tropical Cyclones that Occur in the Western North Pacific Ocean?

Ki-Beom Kim[1,2], Jung-Hee Kim[1,2], Heon-Young Chang[1,2†]

[1]Department Astronomy and Atmospheric Sciences, Kyungpook National University, Daegu 41566, Korea
[2]Research and Training Team for Future Creative Astrophysicists and Cosmologists (BK21 Plus Program)

Understanding solar influences on extreme weather is important. Insight into the causes of extreme weather events, including the solar-terrestrial connection, would allow better preparation for these events and help minimize the damage caused by disasters that threaten the human population. In this study, we examined category three, four, and five tropical cyclones that occurred in the western North Pacific Ocean from 1977 to 2016. We compared long-term trends in the positions of tropical cyclone occurrence and development with variations of the observed sunspot area, the solar North-South asymmetry, and the southern oscillation index (SOI). We found that tropical cyclones formed, had their maximum intensity, and terminated more northward in latitude and more westward in longitude over the period analyzed; they also became stronger during that period. It was found that tropical cyclones cannot be correlated or anti-correlated with the solar cycle. No evidence showing that properties (including positions of occurrence/development and other characteristics) of tropical cyclones are modulated by solar activity was found, at least not in terms of a spectral analysis using the wavelet transform method.

Keywords: solar activity, tropical cyclone, data analysis

1. INTRODUCTION

There is growing evidence that solar activity is related to terrestrial weather and climate (Svensmark & Friis-Christensen 1997; Tinsley 2000; Roldugin & Tinsley 2004; Scafetta & West 2006; Burns et al. 2007; Haigh 2007; Burns et al. 2008; Cho & Chang 2008; Kniveton et al. 2008; Meehl et al. 2009; Gray et al. 2010; Cho et al. 2012; Gray et al. 2017; Lee & Yi 2018; Muraki 2018). Solar signals are statistically associated with synoptic scale variations; some examples include the El Niño-Southern Oscillation (ENSO) (e.g., van Loon et al. 2007; Meehl et al. 2008; van Loon & Meehl 2008; Meehl et al. 2009; Roy & Haigh 2010; Zhou & Tung 2010; Haam & Tung 2012; Roy & Haigh 2012), the quasi biennial oscillation (QBO) (Labitzke 1987; Labitzke & van Loon 1988; Sagir et al. 2015), and the North Atlantic oscillation (NAO) (Gray et al. 2013). Research has shown that the Earth's climate system shows rhythms of the 11 yr solar cycle (Mazzarella &

Palumbo 1992; Kavlakov 2005; Park & Chang 2013), Hale's 22 yr cycle or the 18.6 yr lunar nodal cycle (Hodell et al. 2001; Hwang et al. 2005), and variations of even longer periods (Landscheidt 2000; Bettolli et al. 2010). Solar activity cycles seem to be linked with the climate variability on the Earth via changes in extreme ultraviolet (EUV) irradiance (Gray et al. 2017), the Earth's magnetic/electric fields (Burns et al. 2007, 2008), galactic cosmic rays (GCRs) (Tinsley & Deen 1991; Pudovkin et al. 1997; Marsh & Svensmark 2000; Pudovkin 2004; Roldugin & Tinsley 2004; Haigh 2007; Bazilevskaya et al. 2008), solar energetic particle (SEP) events (Veretenenko & Thejll 2004; Mironova et al. 2012; Mironova & Usoskin 2013, 2014), interplanetary magnetic fields (Tinsley & Heelis 1993; Lam et al. 2013), or high speed solar winds (Zhou et al. 2016).

The impact of solar activity on extreme weather events, such as storms, droughts, and heatwaves, is considered crucial since extreme weather could cause serious natural disasters

that threaten the human population. Solar influences on drought in the Korean peninsula during the period from 1913 to 2012 have been investigated by Park & Chang (2013) and Park et al. (2014). The statistical behavior of tropical storms in the western North Pacific was investigated to determine if there was a correlation with sunspot numbers (Kim et al. 2017). In their study, Kim et al. (2017) reported that, in the solar maximum periods (as compared with the solar minimum periods), tropical cyclones tend to form in the lower latitudes, reach their maximum strength in the lower latitudes, and finish their lives as tropical storms in the lower latitudes. Tropical cyclones occurring in the solar maximum periods also tend to form more eastward in longitude, reach their maximum strength more eastward in longitude, but end their lives as tropical storms more westward in longitude. Furthermore, tropical cyclones have somewhat higher maximum sustained surface wind speed during the solar maximum periods. Based on what they found, Kim et al. (2017) suggested that tropical cyclones occurring in the solar maximum periods and in the solar descending periods resemble those in the El Niño periods in their statistical properties.

Concerns about tropical cyclone activity have led to several theoretical and observational studies (Shen et al. 2000; Emanuel 2005; Trenberth 2005; Webster et al. 2005; Yoshimura & Matsumura, 2005; Gualdi et al. 2008; Zhao et al. 2009; Bender et al. 2010; Yamada et al. 2010; Gleixner et al. 2014; Scoccimarro et al. 2014). The detection of long-term trends in tropical cyclone activity has been a subject of interest (e.g., Camargo & Sobel 2005; Sobel et al. 2016). Regarding storm tracking in the Northern Hemisphere, mid-latitude tropical cyclone activity tends to be decreasing, and high-latitude cyclone activity tends to be increasing (Kossin et al. 2014, 2016). More recently, Kossin (2018) further explored comprehensive data sets and reported that the tropical-cyclone translation speed decreased globally by 10 % over the period from 1949 to 2016. He has suggested that such a decrease is due to global warming with a weakening of summertime tropical circulation.

Motivated by this latest claim and to see if there are trends similar to those Kossin (2018) reported, we examined locations where tropical cyclones form in the western North Pacific Ocean, reach their lowest central pressure, and downgrade back to a tropical depression. Unlike most of the previous studies, where the focus was primarily on the number and/or intensity of tropical cyclones, we examined the locations of tropical cyclone occurrence/development; these locations reflect a decrease or increase in recent tropical cyclone exposure in different regions and the likelihood that these storms threaten the human population. We also compared long-term trends in locations of tropical cyclone occurrence with variations of observed sunspot locations, the solar North-South asymmetry, and the southern oscillation index (SOI). The SOI is defined by an anomaly in the surface air pressure between Tahiti in the Pacific Ocean and Darwin in the Indian Ocean. For comparison, we calculated the linear correlation coefficient r between locations of tropical cyclones and the following data: total sunspot area, the solar North-South asymmetry, and the SOI. Secondly, we computed the power spectrum using the wavelet transform. By doing so, we hoped to find an imprinted signature that solar activity has an impact on the formation of a tropical cyclone as Kim et al. (2017) did. This paper is organized as follows. We begin with descriptions of the analyzed data and methods in Section 2. We discuss annual variations in tropical cyclone occurrence/development in Section 3 and spectral properties of tropical cyclones in Section 4. Finally, we briefly conclude in Section 5.

2. DATA

For the current analysis we used the best track data for category three, four, and five tropical storms that occurred in the western North Pacific Ocean from 1977 to 2016; data was extracted from the Regional Specialized Meteorological Center[1] (RSMC) in Tokyo where detailed data of tropical storms can be downloaded as text files. The data set contains center positions (latitude and longitude in tenths of degrees) at 00:00, 06:00, 12:00, and 18:00 universal time coordinated (UTC), the category of the storm, the maximum sustained surface wind speed (10 min averaged in knots), radii of winds of 30 knots (50 knots) or greater in nautical miles, and central pressures in hPa. As a result, we had data for 1,021 tropical storms. We decided to concentrate on tropical cyclones in the western North Pacific partly be-cause this region has a higher frequency of storms than any other tropical cyclone genesis basin and partly because these storms are likely to directly affect the Korean peninsula. We also utilized updated sunspot area data from the NASA website[2], which is managed by the Marshall Space Flight Center. We extracted the sunspot area data (in units of millionths of a hemisphere) from the same period in which we analyzed tropical storms (from solar cycle 21 to solar cycle 24). The entire sunspot dataset is available as ASCII files; the files are separated into the northern hemisphere

---

and the southern hemisphere. For the SOI, we downloaded data from the NOAA website[3]; this date provides various indices to study large-scale anomalies in space and time that control the variability of the atmospheric circulation.

The wavelet transform can yield the power as a function of both time (distance) and frequency (wave number). The wavelet transform is related to the Fourier transform and the Gabor transform as explained below. The Gabor transform, *GT*, is a function of two parameters: the time, t_0, and frequency, *v*. The Gabor transform is defined as

$$GT(v,t_0) = \int S(t)G(t-t_0)e^{-i2\pi v(t-t_0)}dt \qquad (1)$$

where *S(t)* is the signal and *G(t)* is the running temporal window. In effect, the Gabor transform is a harmonic analysis with a running window centered at a the time t_0. This is simply the Fourier transform with a window, therefore the Gabor transform is a good mathematical microscope that can be used to increase the spatial resolution as one wishes for increasingly small scale variations. The wavelet transform, *WT*, then can be considered as the transform of a signal from an original wavelet by a dilation in time. That is, it is defined

$$WT(d,t_0) = \int S(t)W\left(\frac{t-t_0}{d}\right)dt \qquad (2)$$

where *d* is a dilation coefficient. Like the Gabor transform, the wavelet transform depends on two parameters: the time, t_0, and the dilation coefficient, *d*. Hence, in the power spectrum of the wavelet transform, the information on the power of a signal is displayed in two-dimensional plots, showing variations of the power both with time *(t)* and frequency (*v*=1/*d*).

3. ANNUAL VARIATIONS OF TROPICAL CYCLONES

In Fig. 1, we show the translation speed of category three, four, and five tropical cyclones that occurred in the western North Pacific Ocean from 1977 to 2016. Solid and dashed lines represent the mean annual translation speed of the tropical cyclones as a function of time and the best fit of a linear function, respectively. During the period of the analysis (1977–2016), a decreasing trend of a few percent is clearly seen. Using just the category five tropical cyclone data gave similar results. This finding agrees with what Kossin (2018) has consistently observed in his analysis of datasets during the period from 1949 to 2016, in which trop-
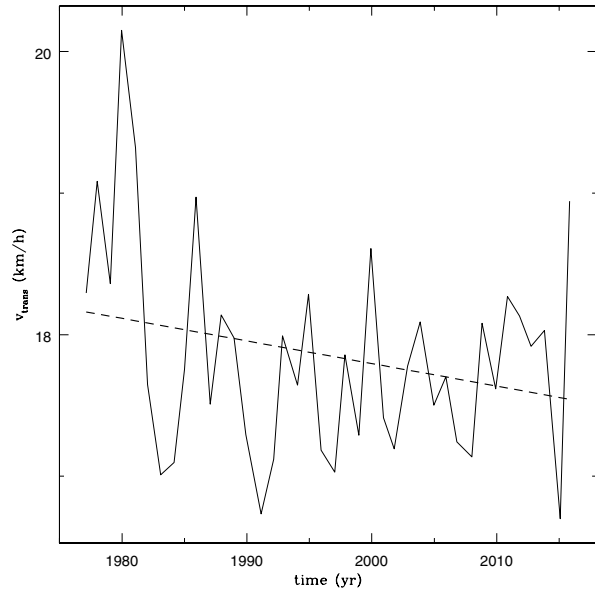
Fig. 1. Translation speed of category three, four, and five tropical cyclones occurring in the western North Pacific Ocean from 1977 to 2016. Solid and dashed lines represent the annual mean translation speed as a function of time and the best fit of a linear function, respectively.

ical cyclones were investigated for the individual ocean basins, over land and water, for the northern and southern hemisphere, and in total. His results also suggest that the rate of the slowdown also varies by longitude and latitude.

In Fig. 2, from top to bottom, we see the variation of latitudes for the following characteristics: where the tropical cyclones formed, where their central pressure became the lowest, and where they were terminated, respectively. A tropical depression is finally designated as a tropical cyclone when its maximum sustained wind speed exceeds 17 m/s for the first time. Similarly, a tropical cyclone is considered as finished when its maximum sustained wind speed goes below 17 m/s from a higher speed than 17 m/s. Solid and dashed lines represent the mean annual latitude as a function of time and the best fit of a linear function, respectively. Plots use data from category three, four, and five tropical cyclones that occurred in the western North Pacific Ocean. During the period of the analysis (1977–2016), the latitudes are slightly increasing. Notably, the rate increase of the latitude where tropical cyclones are terminated is the largest. Using just the category five tropical cyclone data gave similar results. This finding agrees with previous studies that reported a poleward shift in the average latitude where tropical cyclones reach their peak intensity over the past decades (e.g., Trenberth et al. 2005; Kossin et al. 2014). The poleward shifting tendency can be a consequence of the weakening of the steering flow in the tropics (Oey & Chou 2016).
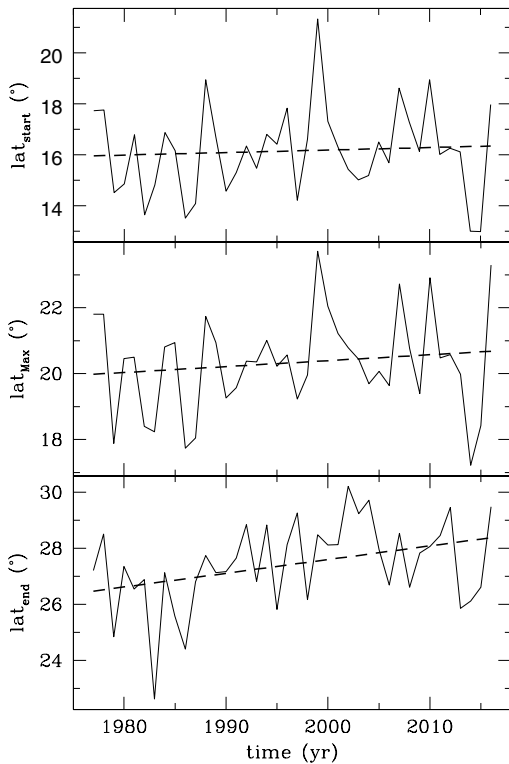
Fig. 2. Variation of latitudes where tropical cyclones formed, where the central pressure became the lowest, and where they were terminated, from top to bottom. Solid and dashed lines represent the annual mean latitude as a function of time and the best fit of a linear function, respectively. Results are from category three, four, and five tropical cyclones occurring in the western North Pacific Ocean from 1977 to 2016.
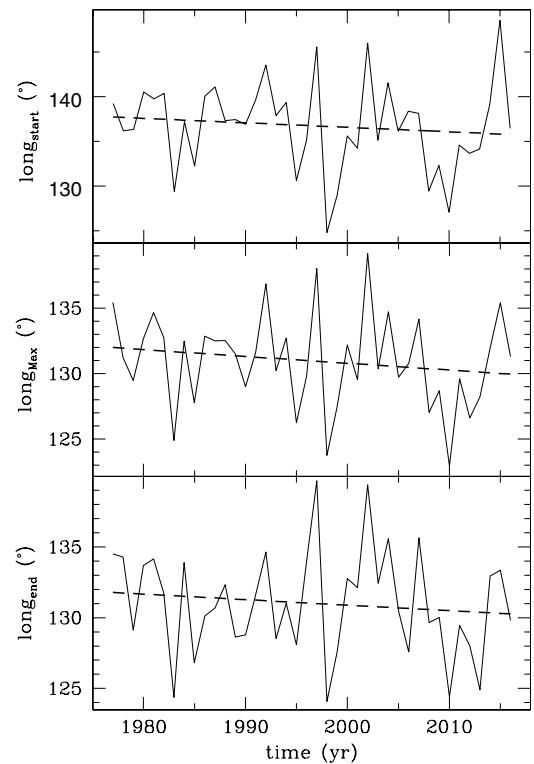
Fig. 3. Variation of longitudes where tropical cyclones formed, where the central pressure became the lowest, and where they were terminated, from top to bottom, respectively. Solid and dashed lines represent the annual mean longitude as a function of time and the best fit of a linear function, respectively. Results are from category three, four, and five tropical cyclones occurring in the western North Pacific Ocean from 1977 to 2016.

In Fig. 3, from top to bottom, we see the variation of longitudes for the following characteristics: where the tropical cyclones formed, where their central pressure became the lowest, and where they were terminated, respectively. Solid and dashed lines represent the mean annual longitude as a function of time and the best fit of a linear function, respectively. Plots use data from category three, four, and five tropical cyclones that occurred in the western North Pacific Ocean. During the period of analysis (1977–2016), the longitudes are slightly decreasing. This means that the location where tropical cyclones formed gradually shifted west with time. Subsequently, the location where they reached their maximum intensity and end of life gradually shifted west with time as well. Again, using just the category five tropical cyclone data gave similar results. This may have implications for the east-west shift of the tropical upper tropospheric trough that controls the longitude of tropical cyclogenesis (e.g., Wu et al. 2015).

In Fig. 4, we show the variation of the lowest central pressure and the maximum sustained wind speed of tropical cyclones in the upper and lower panels, respectively. Solid and dashed lines represent the mean annual pressure and speed as a function of time and the best fit of a linear function, respectively. Plots use data from category three, four, and five tropical cyclones that occurred in the western North Pacific Ocean. A slight decreasing trend in the upper panel and a corresponding increasing trend in the lower panel are seen. While the average translation speed of tropical cyclones decreased, their average lowest central pressure also decreased and thus their intensity became stronger. Hence, a slower and stronger tropical cyclone has been able to pose a more serious hazard to the human population in recent years. If the atmospheric water vapor capacity of a tropical cyclone is increased as the sea surface temperature is increased, then precipitation rates near the tropical cyclone may also be expected to increase, making the damage from a tropical cyclone worse. More seriously, for category five tropical cyclones, we found the maximum sustained wind speed increasing at a rate of six percent during the period of analysis (1977–2016).

In Fig. 5, from top to bottom, we see the variation of the yearly average of the sunspot area appearing in both

154
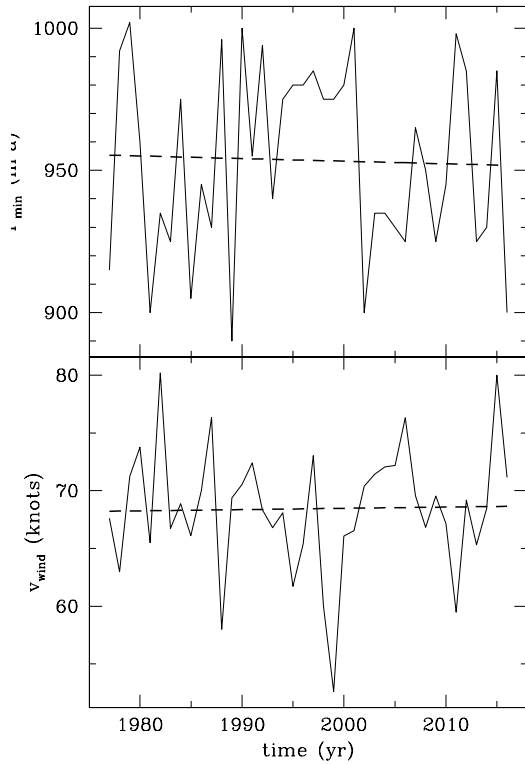
Fig. 4. Variation of the lowest central pressure and the maximum sustained wind speed of tropical cyclones in the upper and lower panels, respectively. Results are the annual averages from category three, four, and five tropical cyclones occurring in the western North Pacific Ocean from 1977 to 2016. Solid and dashed lines represent the annual means as a function of time and the best fit of a linear function, respectively.

Fig. 5. Variation of the yearly average of the total sunspot area, the solar North-South asymmetry, and the SOI, from top to bottom, respectively. Solid and dashed lines represent the annual means as a function of time and the best fit of a linear function, respectively.

the solar northern (A_N) and southern (A_S) hemispheres, the solar North-South asymmetry (which is defined as the difference of the sunspot area appearing in the solar northern and southern hemispheres normalized by their sum, $(A_N-A_S)/(A_N+A_S)$), and the SOI for the period from 1977 to 2016, respectively. When values of the solar North-South asymmetry are positive, the northern solar hemisphere is more active, and vice versa. Solid and dashed lines represent the annual-means as a function of time and the best fit of a linear function, respectively. Interestingly, the annual average of the sunspot area (which indicates the level of the solar magnetic activity cycle) decreased, which may mean that we are living in a descending phase of the modern maximum in a long-term timescale. On the contrary, the average SOI is increasing and even becoming positive. Note that when the El Niño episodes prevail, the SOI is negative, and vice versa.

We calculated a linear correlation coefficient, r, between the specific latitudes, longitudes and other properties of category three, four, and five tropical cyclones occurring in the western North Pacific Ocean, and the solar parameters
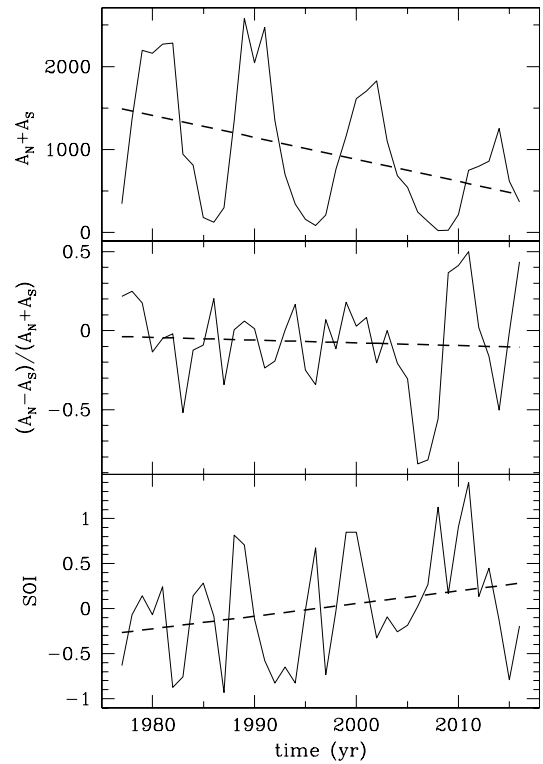
shown in Fig. 5. The solar parameters include the total sunspot area, the solar North-South asymmetry, and the SOI. In Table 1, the correlation coefficient is provided with the single-sided chance probability that $|r|$ has an equal or larger value than its observed value in the null hypothesis. As shown in Table 1, the translation speed of tropical cyc-

Table 1. A linear correlation coefficient, r, and the single-sided chance probability that $|r|$ has an equal or larger value than its observed value in the null hypothesis, P, in parenthesis. This shows the relationship between (1) the total sunspot area ((A_N+A_S)), (2) the solar North-South asymmetry ($(A_N-A_S)/(A_N+A_S)$), and (3) the SOI and positions of tropical cyclone occurrence/development and other cyclone characteristics

	(A_N+A_S)	$(A_N-A_S)/(A_N+A_S)$	SOI
SOI	0.175(0.00)	-0.048(0.06)	---(---)
V_{trans}	0.336(0.00)	0.215(0.00)	0.206(0.00)
P_{min}	0.209(0.00)	0.015(0.31)	0.119(0.00)
V_{wind}	-0.253(0.00)	0.069(0.01)	-0.597(0.00)
lat_{start}	0.122(0.00)	-0.145(1.64)	0.606(0.00)
lat_{Max}	0.213(0.00)	-0.064(0.01)	0.532(0.00)
lat_{end}	0.217(0.00)	0.002(0.48)	0.103(0.00)
$long_{start}$	-0.115(0.00)	0.233(0.00)	-0.567(0.00)
$long_{Max}$	-0.121(0.00)	0.226(0.00)	-0.433(0.00)
$long_{end}$	-0.118(0.00)	0.153(0.00)	-0.260(0.00)

lones, their lowest central pressure, the latitude where the lowest central pressure occurs, and the latitude where the cyclones are terminated are weakly correlated with the total sunspot area, while their maximum sustained wind speed is weakly anti-correlated with the total sunspot area. The translation speed, longitude where the tropical cyclones form, and longitude where the central pressure becomes the lowest are only weakly correlated with the solar North-South asymmetry. The translation speed, latitude where the tropical cyclones form, and latitude where the central pressure becomes the lowest are marginally correlated with the SOI. On the other hand, the maximum sustained wind speed and the longitudes where tropical cyclones form, central pressure becomes the lowest, and the cyclones are terminated are marginally anti-correlated with the SOI. Therefore, we conclude that category three, four, and five tropical cyclones occurring in the western North Pacific Ocean from 1977 to 2016 cannot be correlated or anti-correlated with the solar cycle. However, some parameters of same tropical cyclones are marginally correlated or anti-correlated with the SOI. We repeated the same calculations using only the category five tropical cyclone data and found similar results.

4. SPECTRAL PROPERTIES OF TROPICAL CYCLONE

In Fig. 6, from top to bottom, we show the results of the wavelet transform analysis using the yearly average of the total sunspot area, the solar North-South asymmetry, and the SOI, respectively. The horizontal axis represents time in years starting from 1977, and the vertical axis is the cyclic frequency in $\frac{1}{yr}$. The power is shown in gray scale, which is scaled by the mean value of the noise so that the signal-to-noise ratio can be assessed. In the top panel, the dominant peak at approximately $0.09 \frac{1}{yr}$ in the power spectrum of the sunspot area, corresponding to approximately 11 yr, can be obviously noticed. Note that shorter periodicities, such as, ~5 yr, cannot be seen in this power spectrum simply because the signal-to-noise ratio of the main peak is dominantly large. Bearing in mind that one of the main advantages of the wavelet transform is to yield the variation of the power at a frequency as a function of time, the power at approximately $0.09 \frac{1}{yr}$ is likely present for the period from 1977 to 2016. On the other hand, looking at the results from the solar North-South asymmetry (shown in the middle panel), besides the main peak at approximately $0.09 \frac{1}{yr}$, another peak at approximately $0.125 \frac{1}{yr}$, corresponding to approximately 8 yr, is also seen. Looking at the results from the SOI (shown in the
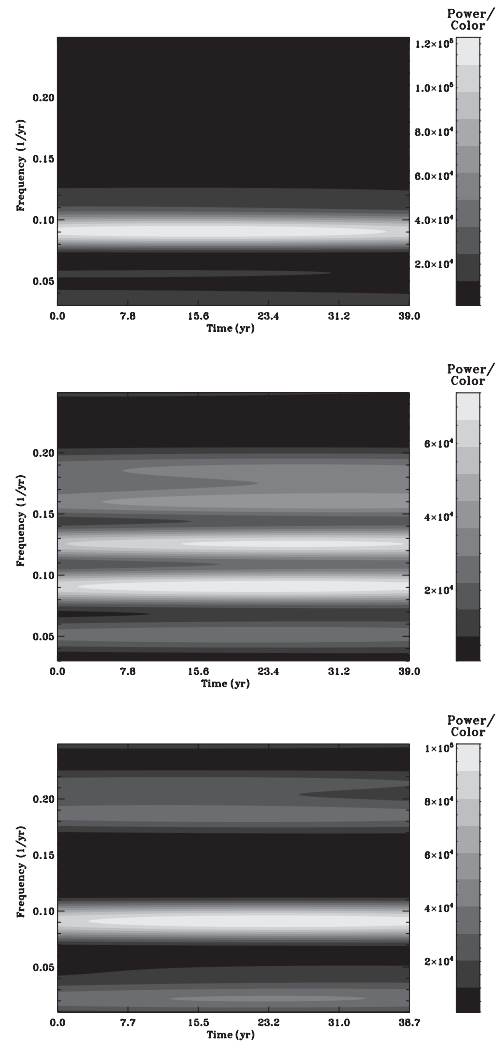
Fig. 6. Wavelet transform analysis from the yearly average of the sunspot area, the solar North-South asymmetry, and the SOI, from top to bottom, respectively. The horizontal axis represents time in years counting starting from 1977, and the vertical axis represents the cyclic frequency in 1/yr. The power is shown in gray scale, which is scaled by the mean value of the noise so that the signal-to-noise ratio can be assessed.

bottom panel), we see not only the dominant peak appearing at approximately $0.09 \frac{1}{yr}$ but also another peak can be found at approximately $1.185 \frac{1}{yr}$, corresponding to approximately 5.4 yr, with magnitudes similar to the signal-to-noise ratio. According to our wavelet transform analysis, the SOI seems to share spectral features with the 11 yr solar cycle. Even though they may share spectral features, this does not mean that the 11 yr solar cycle drives the ENSO. To understand the causal connection between these two, further theoretical examinations are demanded.

In Fig. 7, from top to bottom, we show the results of the wavelet transform analysis from data employed for the plots shown in Fig. 2. The horizontal axis represents time in

years starting from 1977, and the vertical axis represents the cyclic frequency in $\frac{1}{yr}$. The top panel uses the data from the latitudes where tropical cyclones formed. Here, even though the 11 yr periodicity is seen, it is inconspicuous. The main peak appears at approximately 0.04 $\frac{1}{yr}$, corresponding to approximately 25 yr. This might be due to the Pacific Decadal Oscillation (described as a long-lived El Niño-like pattern of Pacific climate variability) or the multi-decadal modulations of the multivariate ENSO Index. In the middle and bottom panels, which show results from latitudes where the central pressure becomes the lowest and where the cyclones are terminated, similar features are observed in the power spectra seen in the top panel. Based on our results, we consider that variations in latitudes of tropical cyclones

are not noticeably modulated by solar activity. We suspect that even a peak with a periodicity of 11 yr may have nothing to do with the 11 yr solar cycle. In Fig. 8, from top to bottom, we show the results of the wavelet transform analysis from data employed for plots shown in Fig. 3. The horizontal axis represents time in years starting from 1977, and the vertical axis represents the cyclic frequency in $\frac{1}{yr}$. The power is shown in gray scale. Features in all power spectra shown here appear the same as in Fig. 7. As discussed in Fig. 7, we consider that variations in longitude of tropical cyclones are not noticeably modulated by solar activity. In Fig. 9, from top to bottom, we show the results of the wavelet transform analysis from the translation speed of tropical cyclones, the lowest central pressure, and the maximum sustained
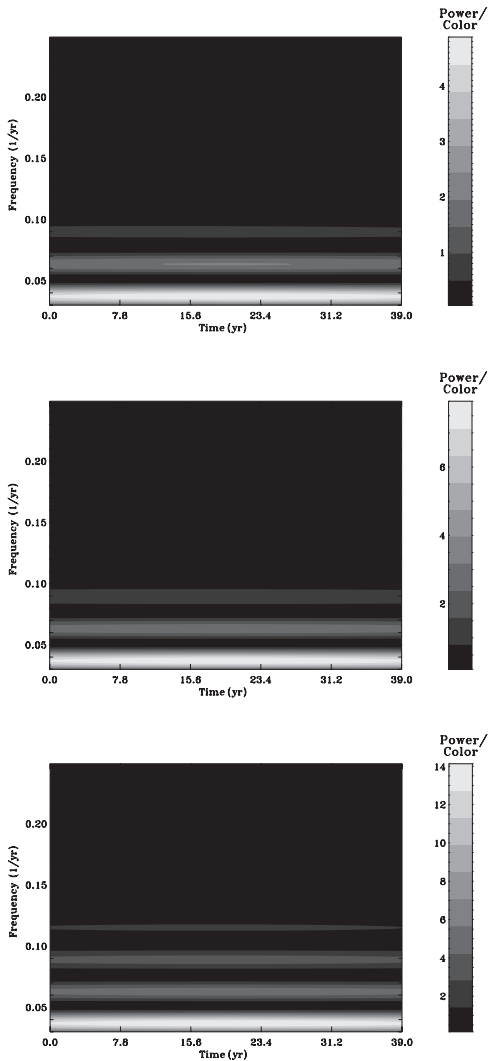
Fig. 7. Plots similar to those in Fig. 6, except resulting from the data shown in Fig. 2 (Latitudes where tropical cyclones formed, where the central pressure became the lowest, and where they were terminated, from top to bottom, respectively).
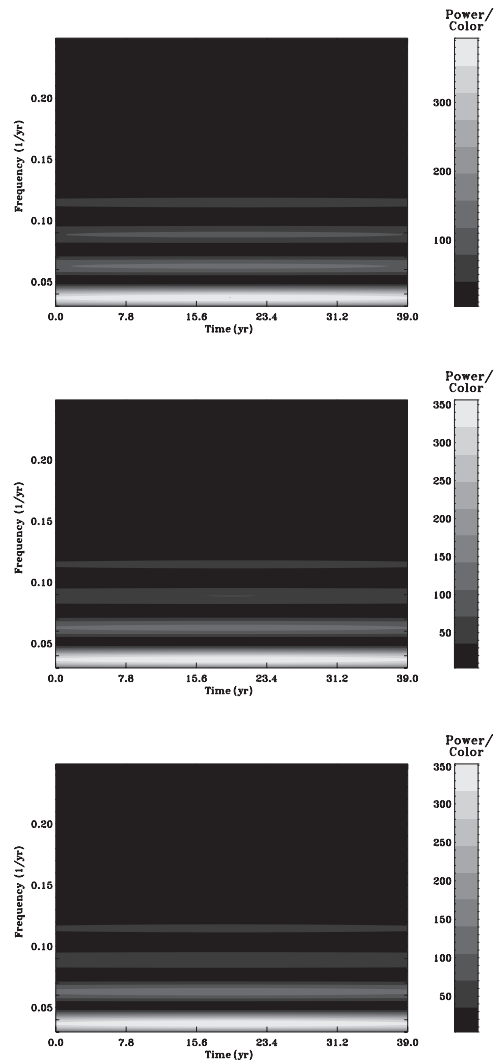
Fig. 8. Plots similar to those in to Fig. 6, except resulting from the data shown in Fig. 3 (Longitudes where tropical cyclones formed, where the central pressure became the lowest, and where they were terminated, from top to bottom, respectively).
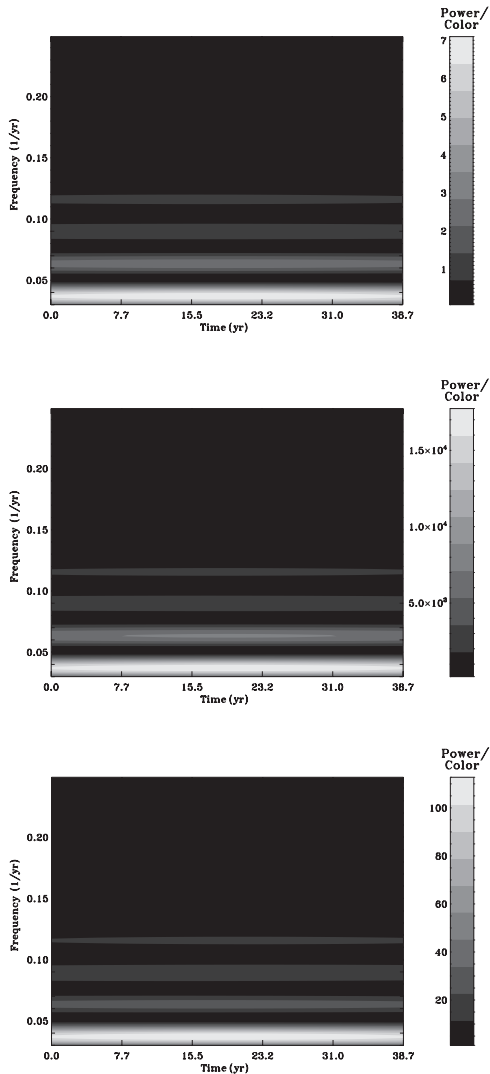
Fig. 9. Plots similar to those in Fig. 6, except resulting from the translation speed of tropical cyclones, their lowest central pressure, and their maximum sustained wind speed, from top to bottom, respectively.

wind speed of the tropical cyclones, respectively. The power spectra all appear the same as in Fig. 7 or Fig. 8. No evidence showing that properties of tropical cyclones are modulated by solar activity was found, at least not in terms of a spectral analysis using the wavelet transform method.

5. SUMMARY AND CONCLUSIONS

The sunspot cycle is known to be related to the terrestrial weather and climate. Solar influences on extreme weather are particularly crucial because the Sun may play a role in recently accelerated global-warming. A better understanding of the causes of extreme weather events including the solar-

terrestrial connection is highly desired to prepare for and minimize the damage of disasters threatening the human population. In addition to discussing several studies on tropical cyclones, we have attempted to explore positions of tropical cyclone occurrence/development and other cyclone characteristics. In this paper, we have examined category three, four, and five tropical cyclones occurring in the western North Pacific Ocean from 1977 to 2016 to determine if there is a general trend over this period and to compare long-term trends in positions of tropical cyclone occurrence with those in variations of the observed sunspot area, the solar North-South asymmetry, and SOI.

Our main findings are as follows:

(1) Latitudes where tropical cyclones formed, where their central pressure became the lowest, and where they terminated increased. The latitude where the tropical cyclones terminated increased the most. Longitudes where tropical cyclones form, where the central pressure became the lowest, and where they terminated decreased such that they appeared more westward in longitude. The lowest central pressure of tropical cyclones has become lower and thus their intensity has become stronger. If the atmospheric water vapor capacity of a tropical cyclone is increased, then precipitation rates near the tropical cyclone may be also expected to increase making the damage from a tropical cyclone worse. The annual average of the total sunspot area is in general decreasing, and the SOI is increasing.

(2) Tropical cyclones cannot be correlated or anti-correlated with the solar cycle. However, some parameters of same tropical cyclones are marginally correlated or anti-correlated with the SOI.

(3) The power spectrum of the SOI using wavelet analysis shows not only the dominant peak appearing at approximately $0.09 \frac{1}{yr}$, corresponding to approximately 11 yr, but also another peak at approximately $1.185 \frac{1}{yr}$, corresponding to approximately 5.4 yr. To study the causal connection between these two results, further theoretical examinations are needed. No evidence showing that properties of tropical cyclones are modulated by solar activity was found, at least not in terms of a spectral analysis using the wavelet transform method. They show rather a periodicity of approximately 25 yr, which could be due to the Pacific Decadal Oscillation or the multi-decadal mod-ulations of the Multivariate ENSO Index.

ACKNOWLEDGMENTS

REFERENCES

Bazilevskaya GA, Usoskin IG, Flückiger EO, Harrison RG, Desorgher L, et al., Cosmic ray induced ion production in the atmosphere, Space Sci. Rev. 137, 149-173 (2008). https://doi.org/10.1007/s11214-008-9339-y

Bender FAM, Ekman AML, Rodhe H, Response to the eruption of Mount Pinatubo in relation to climate sensitivity in the CMIP3 models, Clim. Dyn. 35, 875-886 (2010). https://doi.org/10.1007/s00382-010-0777-3

Bettolli ML, Penalba OC, Vargas WM, Synoptic weather types in the south of South America and their relationship to daily rainfall in the core production region of crops in Argentina, Aust. Meteorol. Oceanogr. J. 60, 37-48 (2010). https://doi.org/10.22499/2.6001.004

Burns AG, Solomon SC, Wang W, Killeen TL, The ionospheric and thermospheric response to CMEs: challenges and successes, J. Atmos. Sol.-Terr. Phys. 69, 77-85 (2007). https://doi.org/10.1016/j.jastp.2006.06.010

Burns AG, Zeng Z, Wang W, Lei J, Solomon SC, et al., Behavior of the F_2 peak ionosphere over the South Pacific at dusk during quiet summer conditions from COSMIC data, J. Geophys. Res. 113, A12305 (2008). https://doi.org/10.1029/2008JA013308

Camargo SJ, Sobel AH, Western North Pacific tropical cyclone intensity and ENSO, J. Clim. 18, 2996-3006 (2005). https://doi.org/10.1175/JCLI3457.1

Cho IH, Chang HY, Long term variability of the sun and climate change, J. Astron. Space Sci. 25, 395-404 (2008). https://doi.org/10.5140/JASS.2008.25.4.395

Cho IH, Kwak YS, Chang HY, Cho KS, Kim YH, et al., The global temperature anomaly and solar North-South asymmetry, Asia-Pac. J. Atmos. Sci. 48, 253-257 (2012). https://doi.org/10.1007/s13143-012-0025-3

Emanuel K, Increasing destructiveness of tropical cyclones over the past 30 years, Nature 436, 686-688 (2005). https://doi.org/10.1038/nature03906

Gleixner S, Keenlyside N, Hodges KI, Tseng WL, Bengtsson L, An inter-hemispheric comparison of the tropical storm response to global warming, Clim. Dyn. 42, 2147-2157 (2014). https://doi.org/10.1007/s00382-013-1914-6

Gray LJ, Beer J, Geller M, Haigh JD, Lockwood M, et al., Solar influences on climate, Rev. Geophys. 48, RG4001 (2010). https://doi.org/10.1029/2009RG000282

Gray LJ, Scaife AA, Mitchell DM, Osprey S, Ineson S, et al., A lagged response to the 11 year solar cycle in observed winter Atlantic/European weather patterns, J. Geophys. Res. 118, 13405-13420 (2013). https://doi.org/10.1002/2013JD020062

Gray LJ, Ball W, Misios S, Solar influences on climate over the Atlantic/European sector, AIP Conf. Proc. 1810, 020002 (2017). https://doi.org/10.1063/1.4975498

Gualdi S, Scoccimarro E, Navarra A, Changes in tropical cyclone activity due to global warming: results from a high-resolution coupled general circulation model, J. Clim. 21, 5204-5228 (2008). https://doi.org/10.1175/2008JCLI1921.1

Haam E, Tung KK, Statistics of solar cycle-La Niña connection: correlation of two autocorrelated time series, J. Atmos. Sci. 69, 2934-2939 (2012). https://doi.org/10.1175/JAS-D-12-0101.1

Haigh JD, The sun and the earth's climate, Living Rev. Sol. Phys. 4, 2 (2007). https://doi.org/10.12942/lrsp-2007-2

Hodell DA, Charles CD, Sierro FJ, Late Pleistocene evolution of the ocean's carbonate system, Earth Planet. Sci. Lett. 192, 109-124 (2001). https://doi.org/10.1016/S0012-821X (01)00430-7

Hwang C, Peng MF, Ning J, Luo J, Sui CH, Lake level variations in China from TOPEX/Poseidon altimetry: data quality assessment and links to precipitation and ENSO, Geophys. J. Int. 161, 1-11 (2005). https://doi.org/10.1111/j.1365-246X.2005.02518.x

Kavlakov SP, Global cosmic ray intensity changes, solar activity variations and geomagnetic disturbances as North Atlantic hurricane precursors, Int. J. Mod. Phys. A 20, 6699-6701 (2005). https://doi.org/10.1142/S0217751X0502985X

Kim JH, Kim KB, Chang HY, Solar influence on tropical cyclone in western North Pacific Ocean, J. Astron. Space Sci. 34, 257-270 (2017). https://doi.org/10.5140/JASS.2017.34.4.257

Kniveton DR, Tinsley BA, Burns GB, Bering EA, Troshichev OA, Variations in global cloud cover and the fair-weather vertical electric field, J. Atmos. Sol.-Terr. Phys. 70, 1633-1642 (2008). https://doi.org/10.1016/j.jastp.2008.07.001

Kossin JP, A global slowdown of tropical-cyclone translation speed, Nature 558, 104-107 (2018). https://doi.org/10.

1038/s41586-018-0158-3

Kossin JP, Emanuel KA, Vecchi GA, The poleward migration of the location of tropical cyclone maximum intensity, Nature 509, 349-352 (2014). https://doi.org/10.1038/nature13278

Kossin JP, Emanuel KA, Camargo SJ, Past and projected changes in western North Pacific tropical cyclone exposure, J. Clim. 29, 5725-5739 (2016). https://doi.org/10.1175/JCLI-D-16-0076.1

Labitzke K, Sunspots, the QBO, and the stratospheric temperature in the north polar region, Geophys. Res. Lett. 14, 535-537 (1987). https://doi.org/10.1029/GL014i005p00535

Labitzke K, van Loon H, Associations between the 11-year solar cycle, the QBO and the atmosphere. Part I: the troposphere and stratosphere in the northern hemisphere in winter, J. Atmos. Terr. Phys. 50, 197-206 (1988). https://doi.org/10.1016/0021-9169(88)90068-2

Lam MM, Chisham G, Freeman MP, The interplanetary magnetic field influences mid-latitude surface atmospheric pressure, Environ. Res. Lett. 8, 045001 (2013). https://doi.org/10.1088/1748-9326/8/4/045001

Landscheidt T, Solar Forcing of El Niño and La Niña, Proceedings of the 1st Solar and Space Weather Euroconference, Santa Cruz de Tenerife, Tenerife, Spain, 25-29 Sep 2000.

Lee SS, Yi Y, Pacific equatorial sea surface temperature variation during the 2015 El Niño period observed by advanced very-high-resolution radiometer of NOAA satellites, J. Astron. Space Sci. 35, 105-109 (2018). https://doi.org/10.5140/JASS.2018.35.2.105

Marsh N, Svensmark H, Cosmic rays, clouds, and climate, Space Sci. Rev. 94, 215-230 (2000). https://doi.org/10.1023/A:1026723423896

Mazzarella A, Palumbo F, Rainfall fluctuations over Italy and their association with solar activity, Theor. Appl. Clim. 45, 201-207 (1992). https://doi.org/10.1007/BF00866193

Meehl GA, Arblaster JM, Branstator G, von Loon H, A coupled air-sea response mechanism to solar forcing in the Pacific region, J. Clim. 21, 2883-2897 (2008). https://doi.org/10.1175/2007JCLI1776.1

Meehl GA, Arblaster JM, Matthes K, Sassi F, von Loon H, Amplifying the Pacific climate system response to a small 11-year solar cycle forcing, Science 325, 1114-1118 (2009). https://doi.org/10.1126/science.1172872

Mironova IA, Usoskin IG, Possible effect of extreme solar energetic particle events of September–October 1989 on polar stratospheric aerosols: a case study, Atmos. Chem. Phys. 13, 8543-8550 (2013). https://doi.org/10.5194/acp-13-8543-2013

Mironova IA, Usoskin IG, Possible effect of strong solar energetic particle events on polar stratospheric aerosol: a summary of observational results, Environ. Res. Lett. 9, 015002 (2014). https://doi.org/10.1088/1748-9326/9/1/015002

Mironova IA, Usoskin IG, Kovaltsov GA, Petelina SV, Possible effect of extreme solar energetic particle event of 20 January 2005 on polar stratospheric aerosols: direct observational evidence, Atmos. Chem. Phys. 12, 769-778 (2012). https://doi.org/10.5194/acp-12-769-2012

Muraki Y, Application of a coupled harmonic oscillator model to solar activity and El Niño phenomena, J. Astron. Space Sci. 35, 75-81 (2018). https://doi.org/10.5140/JASS.2018.35.2.75

Oey LY, Chou S, Evidence of rising and poleward shift of storm surge in western North Pacific in recent decades, J. Geophys. Res. 121, 5181-5192 (2016). https://doi.org/10.1002/2016JC011777

Park JH, Chang HY, Drought over Seoul and its association with solar cycles, J. Astron. Space Sci. 30, 241-246 (2013). https://doi.org/10.5140/JASS.2013.30.4.241

Park JH, Kim KB, Chang HY, Statistical properties of effective drought index (EDI) for Seoul, Busan, Daegu, Mokpo in South Korea, Asia-Pac. J. Atmos. Sci. 50, 453-458 (2014). https://doi.org/10.1007/s13143-014-0035-4

Pudovkin MI, Influence of solar activity on the lower atmosphere state, Int. J. Geomagn. Aeron. 5, GI2007 (2004).

Pudovkin MI, Veretenenko SV, Pellinen R, Kyrö E, Meteorological characteristic changes in the high-latitudinal atmosphere associated with Forbush decreases of the galactic cosmic rays, Adv. Space Res. 20, 1169-1172 (1997). https://doi.org/10.1016/S0273-1177(97)00767-9

Roldugin VC, Tinsley BA, Atmospheric transparency changes associated with solar wind-induced atmospheric electricity variations, J. Atmos. Sol.-Terr. Phys. 66, 1143-1149 (2004). https://doi.org/10.1016/j.jastp.2004.05.006

Roy I, Haigh JD, Solar cycle signals in sea level pressure and sea surface temperature, Atmos. Chem. Phys. 10, 3147-3153 (2010). https://doi.org/10.5194/acp-10-3147-2010

Roy I, Haigh JD, Solar cycle signals in the pacific and the issue of timings, J. Atmos. Sci. 69, 1446-1451 (2012). https://doi.org/10.1175/JAS-D-11-0277.1

Sagir S, Karatay S, Atici R, Yesil A, Ozcan O, The relationship between the quasi biennial oscillation and sunspot number, Adv. Space Res. 55, 106-112 (2015). https://doi.org/10.1016/j.asr.2014.09.035

Scafetta N, West BJ, Phenomenological solar contribution to the 1900-2000 global surface warming, Geophys. Res. Lett. 33, L05708 (2006). https://doi.org/10.1029/2005GL025539

Scoccimarro E, Gualdi S, Villarini G, Vecchi GA, Zhao M, et al., Intense precipitation events associated with landfalling tropical cyclones in response to a warmer climate and

increased CO2, J. Clim. 27, 4642-4654 (2014). https://doi.org/10.1175/JCLI-D-14-00065.1

Shen W, Tuleya RE, Ginis I, A sensitivity study of the thermodynamic environment on GFDL model hurricane intensity: Implications for global warming, J. Clim. 13, 109-121 (2000). https://doi.org/10.1175/1520-0442(2000)013<0109:ASSOTT>2.0.CO;2

Sobel AH, Camargo SJ, Hall TM, Lee CY, Tippett MK, et al., Human influence on tropical cyclone intensity, Science 353, 242-246 (2016). https://doi.org/10.1126/science.aaf6574

Svensmark H, Friis-Christensen E, Variation of cosmic ray flux and global cloud coverage-a missing link in solar-climate relationships, J. Atmos. Sol.-Terr. Phys. 59, 1225-1232 (1997). https://doi.org/10.1016/S1364-6826(97)00001-1

Tinsley BA, Influence of solar wind on the global electric circuit, and inferred effects on cloud microphysics, temperature, and dynamics in the troposphere, Space Sci. Rev. 94, 231-258 (2000). https://doi.org/10.1023/A:1026775408875

Tinsley BA, Deen GW, Apparent tropospheric response to MeV-GeV particle flux variations: a connection via electrofreezing of supercooled water in high-level clouds?, J. Geophys. Res. 96, 22283-22296 (1991). https://doi.org/10.1029/91JD02473

Tinsley BA, Heelis RA, Correlations of atmospheric dynamics with solar activity evidence for a connection via the solar wind, atmospheric electricity, and cloud microphysics, J. Geophys. Res. 98, 10375-10384 (1993). https://doi.org/10.1029/93JD00627

Trenberth K, Uncertainty in hurricanes and global warming, Science 308, 1753-1754 (2005). https://doi.org/10.1126/science.1112551

van Loon H, Meehl GA, The response in the pacific to the sun's decadal peaks and contrasts to cold events in the southern oscillation, J. Atmos. Sol.-Terr. Phys. 70, 1046-1055 (2008). https://doi.org/10.1016/j.jastp.2008.01.009

van Loon H, Meehl GA, Shea DJ, Coupled air-sea response to solar forcing in the pacific region during northern winter, J. Geophys. Res. 112, D02108 (2007). https://doi.org/10.1029/2006JD007378

Veretenenko S, Thejll P, Effects of energetic solar proton events on the cyclone development in the North Atlantic, J. Atmos. Sol.-Terr. Phys. 66, 393-405 (2004). https://doi.org/10.1016/j.jastp.2003.11.005

Webster PJ, Holland GJ, Curry JA, Chang HR, Changes in tropical cyclone number, duration, and intensity in a warming environment, Science 309, 1844-1846 (2005). https://doi.org/10.1126/science.1116448

Wu L, Wang C, Wang B, Westward shift of western North Pacific tropical cyclogenesis, Geophys. Res. Lett. 42, 1537-1542 (2015). https://doi.org/10.1002/2015GL063450

Yamada Y, Oouchi K, Satoh M, Tomita H, Yanase W, Projection of changes in tropical cyclone activity and cloud height due to greenhouse warming: Global cloud-system-resolving approach, Geophys. Res. Lett. 37, L07709 (2010). https://doi.org/10.1029/2010GL042518

Yoshimura H, Matsumura T, A two-time-level vertically-conservative semi-Lagrangian semi-implicit double Fourier series AGCM, CAS/JSC WGNE Res. Act. Atmos. Ocean Model. 35, 27-28 (2005).

Zhao M, Held IM, Lin SJ, Vecchi GA, Simulations of global hurricane climatology, interannual variability, and response to global warming using a 50-km resolution GCM, J. Clim. 22, 6653-6678 (2009). https://doi.org/10.1175/2009JCLI3049.1

Zhou J, Tung KK, Solar cycles in 150 years of global sea surface temperature data, J. Clim. 23, 3234-3248 (2010). https://doi.org/10.1175/2010JCLI3232.1

Zhou L, Tinsley B, Chu H, Xiao Z, Correlations of global sea surface temperatures with the solar wind speed, J. Atmos. Sol.-Terr. Phys. 149, 232-239 (2016). https://doi.org/10.1016/j.jastp.2016.02.010